

Oil Filled Flow Shield Performance Evaluation

March 2026

- 1 Emma Cotter (PNNL)
- 2 Spencer Nelson (PNNL)
- 3 Joseph Haxel (PNNL)
- 4 Benjamin Strom (XFlow Energy Company)
- 5 Ian Brownstein (XFlow Energy Company)

DISCLAIMER

This report was prepared as an account of work sponsored by an agency of the United States Government. Neither the United States Government nor any agency thereof, nor Battelle Memorial Institute, nor any of their employees, makes **any warranty, express or implied, or assumes any legal liability or responsibility for the accuracy, completeness, or usefulness of any information, apparatus, product, or process disclosed, or represents that its use would not infringe privately owned rights.** Reference herein to any specific commercial product, process, or service by trade name, trademark, manufacturer, or otherwise does not necessarily constitute or imply its endorsement, recommendation, or favoring by the United States Government or any agency thereof, or Battelle Memorial Institute. The views and opinions of authors expressed herein do not necessarily state or reflect those of the United States Government or any agency thereof.

PACIFIC NORTHWEST NATIONAL LABORATORY
operated by
BATTELLE
for the
UNITED STATES DEPARTMENT OF ENERGY
under Contract DE-AC05-76RL01830

Printed in the United States of America

Available to DOE and DOE contractors from the
Office of Scientific and Technical Information,
P.O. Box 62, Oak Ridge, TN 37831-0062;
ph: (865) 576-8401
fax: (865) 576-5728
email: reports@adonis.osti.gov

Available to the public from the National Technical Information Service
5301 Shawnee Rd., Alexandria, VA 22312
ph: (800) 553-NTIS (6847)
email: orders@ntis.gov <<https://www.ntis.gov/about>>
Online ordering: <http://www.ntis.gov>

Oil Filled Flow Shield Performance Evaluation

March 2026

- 1 Emma Cotter (PNNL)
- 2 Spencer Nelson (PNNL)
- 3 Joseph Haxel (PNNL)
- 4 Benjamin Strom (XFlow Energy Company)
- 5 Ian Brownstein (XFlow Energy Company)

Prepared for
the U.S. Department of Energy
under Contract DE-AC05-76RL01830

Pacific Northwest National Laboratory
Richland, Washington 99354

Abstract

When hydrophones are used to monitor underwater sound in areas with currents, like rivers or tidal channels, flow noise caused by turbulent flow past a hydrophone can mask low frequency acoustic signals of interest. Flow shields can reduce the impacts of flow noise on hydrophone data. A prior study conducted by PNNL compared three flow shield designs and determined that an oil-filled urethane shield performed better than other designs and was likely sufficiently robust for long-duration marine deployments. However, that study did not assess the high frequency performance of the oil-filled flow shield or conduct long-duration field testing. Further, the prototype flow shield was difficult to assemble. This report details the results of design refinement and testing to address these gaps. Design refinements resulted in a straightforward and repeatable assembly method. Field testing indicated that the flow shields reduce flow noise by over 20 dB below 50 Hz at flow speeds greater than 0.5 m/s and are proven to survive deployments more than 6 months long. Calibration of the same hydrophone with and without a flow shield installed indicated that the shields attenuate propagating sound by no more than 2 dB at frequencies below 30 kHz.

Acknowledgments

The authors gratefully acknowledge the contributions of Tristen Myers, Emma Geon, and Linnea Weicht to this work. This work was funded by the U.S. Department of Energy Office of Technology Commercialization through the Technology Commercialization Fund.

Acronyms and Abbreviations

PNNL – Pacific Northwest National Laboratory

XFlow – XFlow Energy Company

ADV – Acoustic Doppler velocimeter

Contents

Abstract.....	ii
Acknowledgments.....	iii
Acronyms and Abbreviations.....	iv
1.0 Introduction	7
2.0 High-frequency performance	9
3.0 Field Testing and Evaluation	11
3.1 Test Configuration and Data Processing.....	11
3.2 Acoustic Results	12
3.3 Durability.....	15
4.0 Ease of Assembly.....	16
5.0 Conclusions.....	17
6.0 References.....	18
Appendix A – Flow Shield Drawing	A.1
Appendix B – Flow Shield Installation Instructions	B.2
Appendix C – Field Test Data Description and Processing	C.3
Appendix D – Hydrophone Calibration Uncertainty	D.4

Figures

Figure 1: icListen hydrophone prior to calibration with each of the three flow shields. Flow shields 1-3 are shown from left to right. Note that the hydrophone housing was coated with white anti-biofouling paint for another project. Photos provided by Ocean Networks Canada.....	9
Figure 2: Top) Calibration curve for one icListen HF RB9 hydrophone without a flow shield (baseline) and with each of the three flow shields shown in Figure 1. Bottom) Difference between the calibration curve with each hydrophone and the unshielded hydrophone (baseline).....	10
Figure 3: Instrumented lander prior to deployment. The hydrophone to the far right did not collect valid data, so all results are from the hydrophones on the right hand side of the lander.....	11
Figure 4: Mean spectra recorded by the baseline hydrophone (B) and the shielded hydrophone (S), binned by flow speed.....	12
Figure 5: 1-minute average band levels and flow speed for a 4-day period. From top to bottom: 20-50 Hz band, 50-80 Hz band, 4000-5000 Hz band, and flow speed measured by the ADV.	Error! Bookmark not defined.
Figure 6: 1-minute average spectra from each hydrophone during two representative periods. Top: peak flow speeds (0.67 m/s), bottom: slack tide	14
Figure 7: Pier-mounted hydrophone with flow shield upon deployment (August 2025) and during diver inspection (March 2026).	15

Figure 8: Dimensioned drawing of the icListen HF flow shield that was tested A.1

Figure 9: Photographs of key installation steps B.2

Figure 10: Timeseries of horizontal flow velocity recorded by the ADV C.3

Figure 11: The same data as shown in Figure 6 before applying calibration curves to
convert to units of pressure D.4

Figure 12: Calibration curves for each hydrophone used in the field trial to convert from
units of V to units of pressure. Calibration curves were measured with no
flow shield attached. D.4

1.0 Introduction

Hydrophones measure underwater sound by sensing the pressure fluctuations associated with propagating sound waves. However, when the surrounding water is moving relative to the hydrophone, hydrophones will also sense non-acoustic pressure fluctuations associated with turbulence in the flow and flow interaction with the hydrophone body. This effect is called flow noise and can mask signals of interest at low acoustic frequencies (<1 kHz). These low frequencies are particularly relevant for many applications of underwater acoustic monitoring because they can propagate over long distances in the ocean and overlap with the hearing range and vocalizations of many marine animals (Haver et al. 2018). Because flow noise increases in amplitude with increasing flow speed, it is a particularly relevant challenge for passive acoustic measurements in rivers or tidal channels with strong currents.

There are two primary approaches to mitigating flow noise. In some cases, flow noise can be reduced or eliminated by affixing hydrophones to drifting buoys, reducing the relative velocity between the hydrophone and the water (e.g., Polagye et al. 2024). However, acoustic surveys with drifting hydrophones typically cannot capture long-term temporal variability in the sound field. The alternative to drifting hydrophones is to use fixed hydrophone systems (e.g., on a lander on the seabed) and mitigate flow noise with a flow shield that reduces the effects of flow noise on the hydrophone. To be effective, a flow shield must reduce flow noise contamination at low frequencies (< 1 kHz) without attenuating propagating sound at higher frequencies (> 1 kHz) or creating other sources of sound that might contaminate recordings, like rattling or flapping. Further, flow shields intended for long-term deployments must not degrade in the marine environment and should be robust to biofouling.

Flow shields have been routinely used by underwater acoustics researchers for decades. However, there are no commercially available flow shields, requiring hydrophone users to design ad-hoc solutions with unquantified effectiveness and reliability. For example, in a study at the Camp Rilea wave energy test site on the coast of northern Oregon, Haxel and Henkel 2017 used thin nylon flow shields that were ineffective in reducing flow noise and created a fluttering sound during strong currents that further contaminated recordings.

To address this, in 2024, Pacific Northwest National Laboratory (PNNL) conducted a side-by-side test of three flow shield designs: an oil-filled urethane enclosure, a thin nylon covering, and a thick ballistic nylon covering. The study found that the oil filled, urethane enclosure, which was manufactured by XFlow, was most effective at reducing flow noise and, unlike the fabric flow shields, it was likely sufficiently robust for long-term deployments (Cotter et al. 2024). While the 2024 study demonstrated the potential of the oil-filled flow shield to improve acoustic measurements in dynamic environments, analysis of high frequency performance was limited to frequencies below 20 kHz, and testing was limited to a one-week field trial. The flow shield was also difficult to assemble; assembly required over-topping the flow shield and spilling oil on the work surface.

Therefore, PNNL and XFlow partnered to refine the design of the oil-filled flow shield and conduct further testing of its performance. This report presents the results of that refinement and testing. While the prior study used Ocean Instruments SoundTrap ST600 HF hydrophones, this study used Ocean Sonics icListen HF hydrophones. This hydrophone was selected to verify if flow shield would be effective with a different hydrophone system. Both hydrophone models (SoundTrap and icListen) are widely used for marine environmental monitoring.

This report addresses three key topics:

1. High-frequency performance
2. Additional field testing
3. Ease of assembly

These topics are discussed in the subsequent sections of this report. Overall, the results indicate that the oil filled flow shield:

- attenuates propagating sound by no more than 2 dB at frequencies below 30 kHz,
- reduces flow noise by over 20 dB below 50 Hz at flow speeds greater than 0.5 m/s,
- is proven to survive deployments more than 6 months long¹, and
- is easy to assemble.

¹ Note that failure was not observed at 6 months, rather this was the maximum test duration possible during the project period.

2.0 High-frequency performance



Figure 1: icListen hydrophone prior to calibration with each of the three flow shields. Flow shields 1-3 are shown from left to right. Note that the hydrophone housing was coated with white anti-biofouling paint for another project. Photos provided by Ocean Networks Canada.

Cotter et al. (2024) found that ambient noise spectra measured during periods of little or no flow noise by a hydrophone with a flow shield and an unshielded hydrophone agreed well below 20 kHz, indicating that the flow shield did not significantly attenuate acoustic frequencies in this range. However, the 2024 study did not evaluate frequencies higher than 20 kHz and did not conduct calibration of hydrophones with the flow shields attached. To address this gap, a hydrophone (icListen HF RB9; serial number 6661) was calibrated with and without a flow shield to compare the resulting calibration curves. This was repeated with three separate flow shields to investigate any manufacturing variability between shields (Figure 1). Calibration was conducted by the Ocean Networks Canada Hydrocal facility (Biffard et al. 2022) from 2 kHz to 130 kHz at 60 linearly spaced frequencies. We note that this test was conducted with same hydrophone as the shielded hydrophone in the field evaluation described in Section 3. Figure 2a shows the calibration curve obtained for the unshielded hydrophone (baseline) and with each flow shield. Figure 2b shows difference between the baseline calibration curve and the calibration curve with each flow shield.

Below 30 kHz, the calibration curves with all three flow shields agree with the baseline calibration curve within 2 dB, indicating minimal attenuation by the flow shield at these frequencies. Above 30 kHz, attenuation up to 6 dB is observed at some frequencies. The calibration curves with flow shields 1 and 3 are within 2.5 dB of each other at all frequencies. Both calibration curves deviate from the baseline calibration by up to 5 dB around 32, 64, and 98 kHz, but show good agreement with the baseline calibration at other frequencies. This can likely be explained by modest attenuation of propagating sound through the oil within the flow shield. The wavelength of sound in seawater at 32 kHz is approximately 47 mm, equivalent to the inner diameter of the flow shield (Appendix A), which likely results in attenuation at this frequency and its multiples (harmonics). This indicates that the frequencies at which attenuation by the flow shield is observed are likely dependent on flow shield geometry and would differ if the diameter of the flow shield changed (e.g., to accommodate a different hydrophone model).

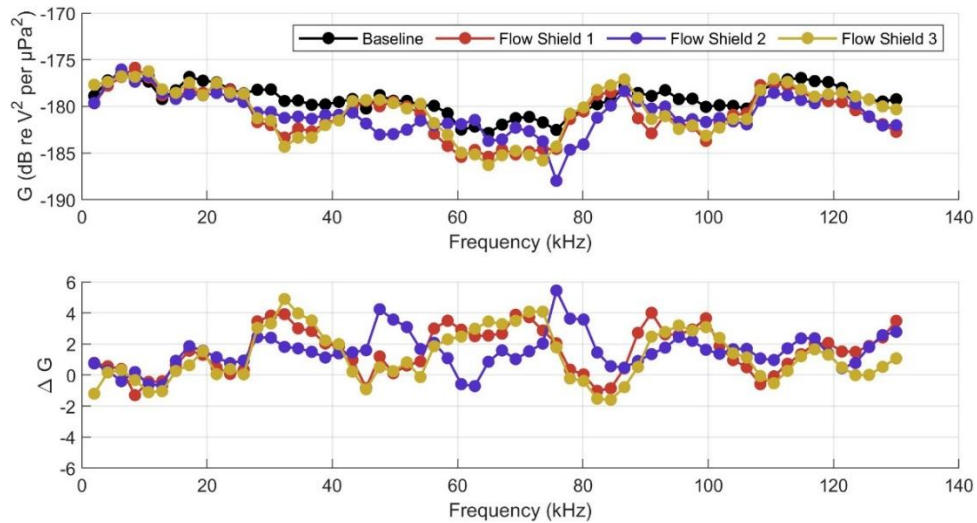


Figure 2: Top) Calibration curve for one icListen HF RB9 hydrophone without a flow shield (baseline) and with each of the three flow shields shown in Figure 1. Bottom) Difference between the calibration curve with each hydrophone and the unshielded hydrophone (baseline)

Flow shield 2 exhibits different trends than flow shields 1 and 3. The calibration curve with flow shield 2 deviates from the baseline calibration curve most significantly near 47 and 75 kHz, and remains within 3 dB of the baseline calibration at other frequencies. The differences between flow shield 2 and flow shields 1 and 3 may be explained by misalignment of flow shield 2 during calibration; Figure 1 indicates that the hydrophone element was less centered in flow shield 2 during calibration. Because the flow shields were disassembled after calibration, it is not possible to further validate this hypothesis, but this result indicates that misalignment during flow shield assembly could result in minor changes in the resulting hydrophone sensitivity.

In summary, the flow shields do not significantly attenuate propagating sound below 30 kHz. Above 30 kHz, up to 6 dB of attenuation is observed in particular frequency bands, likely driven by the geometry of the flow shield. While 6 dB of attenuation is not insignificant, it is small compared to the signal to noise gain achieved with the reduction in flow noise.

3.0 Field Testing and Evaluation

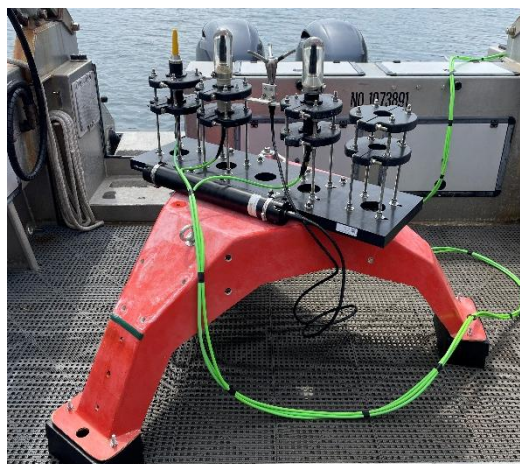


Figure 3: Instrumented lander prior to deployment. The hydrophone to the far right did not collect valid data, so all results are from the hydrophones on the left hand side of the lander.

3.1 Test Configuration and Data Processing

Field testing was conducted at PNNL-Sequim's Marine and Coastal Research Laboratory in the tidal channel at the entrance to Sequim Bay. Three Ocean Sonics icListen HF hydrophones were mounted on a tripod lander with an acoustic Doppler velocimeter (ADV), a similar configuration to the test conducted in Cotter et al. (2024) (Figure 3). Two hydrophones were fitted with flow shields, and the third served as a baseline measurement. Unfortunately, one of the two shielded hydrophones did not collect valid data due to prior damage unrelated to this experiment, so the results presented in this section compare one shielded and one unshielded hydrophone. Both hydrophones were calibrated, without flow shields, at the Ocean Networks Canada HydroCal facility in November 2025; a low frequency calibration was conducted from 0-700 Hz and a high frequency calibration was conducted from 2-130 kHz.

The lander was deployed on the seabed adjacent to PNNL-Sequim's pier for 26 days from June 5 to July 1, 2025. To minimize the effects of turbulence due to flow over adjacent sensors, upon deployment, divers adjusted the lander so that the row of sensors was approximately perpendicular to the dominant direction of the tidal currents. Each hydrophone was configured to collect data continuously with a sample rate of 256 kHz and was cabled to an Ocean Sonics Launch Box on the pier that provided power and wireless data connectivity. Data were stored on the hydrophone's internal storage until periodic offload via the wireless connection.

Data processing for the hydrophone and ADV followed the same methods as in Cotter et al. (2024) with minor modifications to account for the higher sampling rate of the hydrophones, and is summarized in Appendix B. Additionally, 1-minute average band levels were calculated for the 20-50 Hz, 50-80 Hz, and 4000-5000 Hz bands.

3.2 Acoustic Results

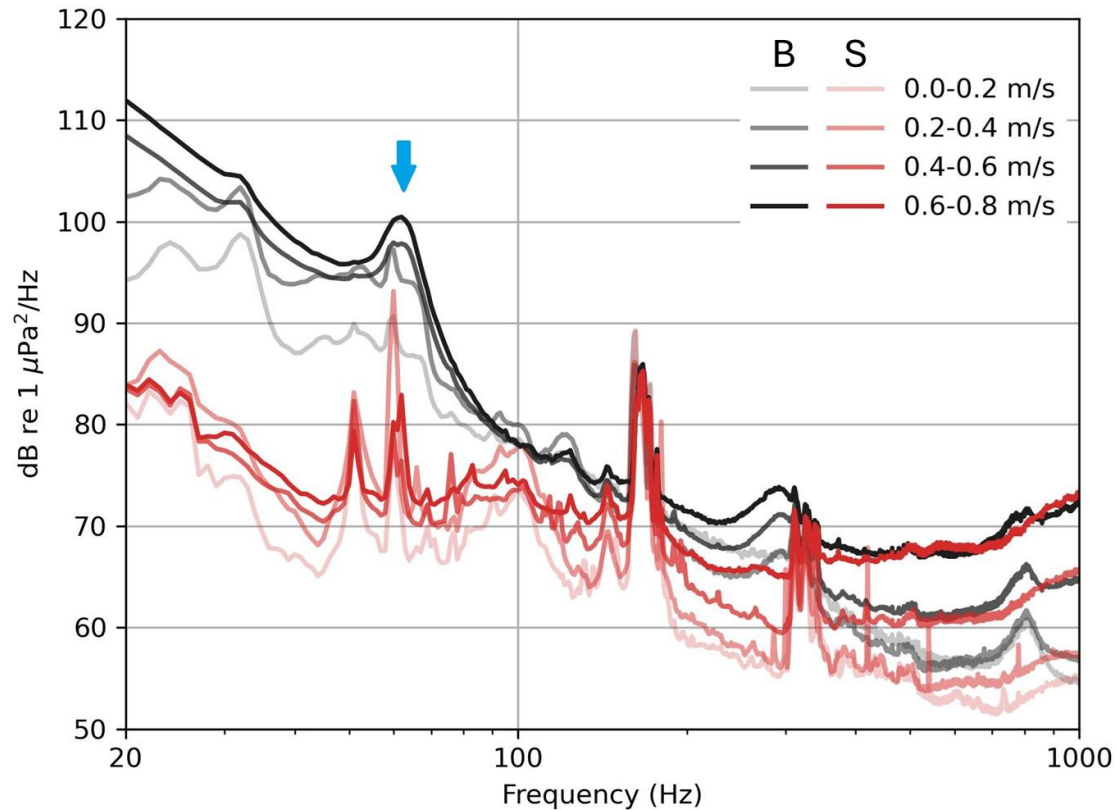


Figure 4: Mean spectra recorded by the baseline hydrophone (B) and the shielded hydrophone (S), binned by flow speed. The blue arrow highlights a tone at approximately 60 Hz that was only faintly detectable by the baseline hydrophone due to flow noise.

Peak horizontal flow speeds reached 0.75 m/s (a full timeseries of flow velocity can be found in Appendix D). Figure 4 shows the mean acoustic power spectral density from each hydrophone in 0.2 m/s water velocity bins from 20 to 1,000 Hz. Flow noise mitigation by the flow shield is evident. Below 200 Hz, noise levels measured by the baseline hydrophone increase with flow speed, while noise levels measured by the shielded hydrophone remain relatively constant. Even in data collected when flow speeds were between 0 and 0.2 m/s, noise levels measured by the baseline hydrophone are elevated over 10 dB above the shielded hydrophone at the lowest frequencies measured. Notably, a tone at 60 Hz, indicated by the blue arrow in Figure 4, is clearly detectable at all flow speeds with the shielded hydrophone, but only faintly detectable in the same conditions with the baseline hydrophone. This tone is likely associated with the nearby water intake for PNNL-Sequim's laboratories. Similarly, the signal to noise ratio of a tone at 160 kHz (also associated with the water intake) is increased by nearly 10 dB in flow speeds below 0.5 m/s. Above approximately 300 Hz, noise levels measured by the baseline and

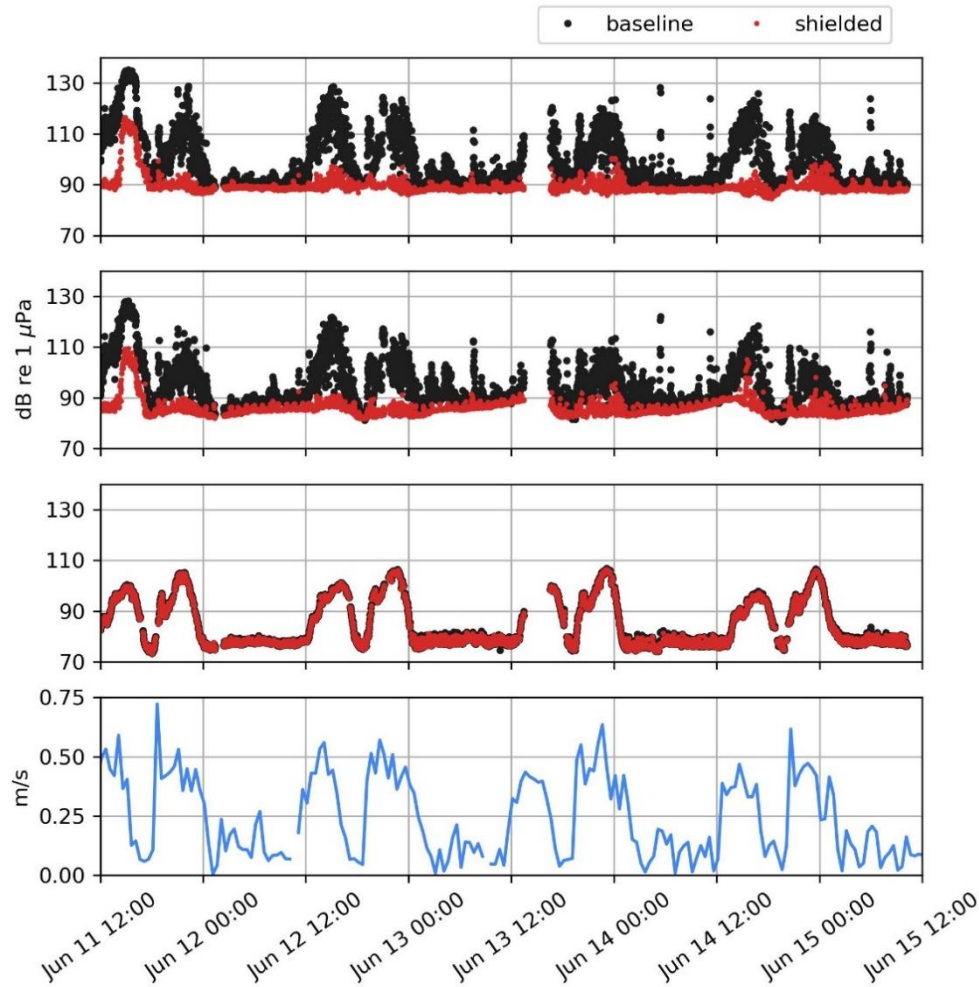


Figure 5: 1-minute average band levels and flow speed for a 4-day period. From top to bottom: 20-50 Hz band, 50-80 Hz band, 4000-5000 Hz band, and flow speed measured by the ADV.

shielded hydrophones agree well, indicating that flow noise did not impact measurements at these frequencies.

Figure 5 shows the 1-min average frequency band sound levels (L_{eq}) from each hydrophone and the corresponding flow speed for a representative 4-day period during the deployment and the corresponding flow speed measured by the ADV. Flow noise contamination, and the resulting reduction in flow noise by the flow shield, is evident in the 20-50 Hz and 50-80 Hz bands. Increases in noise levels during periods of peak flow in the 4-5 kHz band are dominated by sediment generated propagating sound, rather than flow noise (Bassett et al. 2013), and the measurements by the two hydrophones agree well. Variability in the level of flow noise contamination during periods of strong flow is likely the result of a combination of factors. First, the ADV only sampled every 30 minutes, and likely did not capture the peak flow conditions. Second, flow around the research pier results in high levels of turbulence that impact flow noise levels. Finally, while data were manually reviewed to remove periods contaminated by passing vessel traffic or other transient sounds, it is likely that kelp or other debris entangled with the sensors during periods of strong flow, and divers reported crustacea climbing on the

hydrophones. These events may have resulted in low frequency non-acoustic pressure fluctuations measured by the hydrophone.

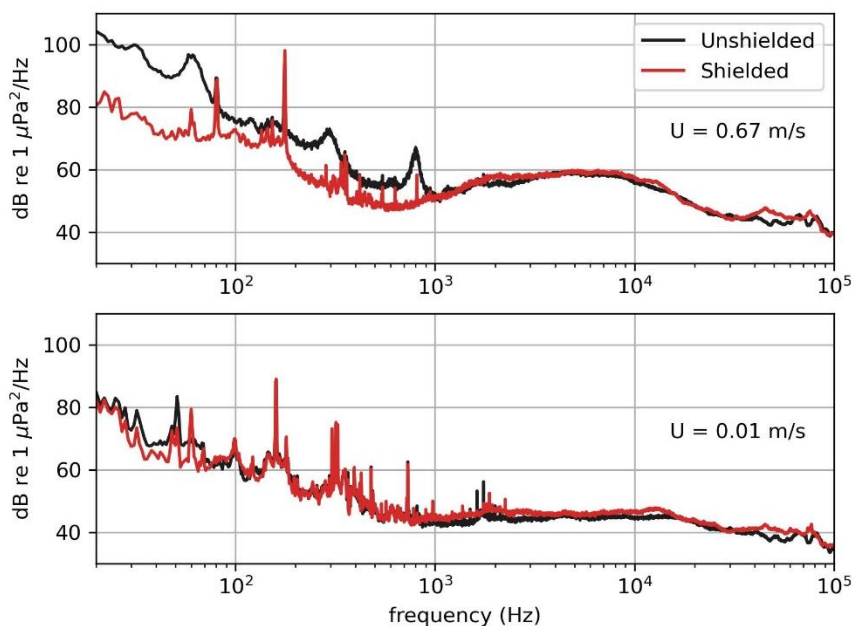


Figure 6: 1-minute average spectra from each hydrophone during two representative periods.
Top: peak flow speeds (0.67 m/s), bottom: slack tide

Figure 6 shows 1-min mean spectra from 20 Hz to 100 kHz from both hydrophones during two periods: during low flow (<0.05 m/s) and during the strongest flow speeds measured during the deployment (>.65 m/s). Several trends can be observed. First, as expected from the calibration results presented in the previous section, the spectra measured by the two hydrophones agree well below approximately 30 Hz during slack tide. However, even in these low flow conditions, noise levels measured by the baseline hydrophone are elevated by several dB below 80 Hz. This can likely be attributed to the fact that the signal to noise ratio of ADV measurements decreases at low flow speeds (below approximately 0.25 m/s), and the limited sampling interval of the ADV did not capture fluctuations in flow speed (i.e., flow speeds were likely higher than 0.01 m/s during the recording period). Above 30 kHz, data from the shielded hydrophone are up to 5 dB higher amplitude than the unshielded hydrophone. This is counterintuitive, as the calibration results presented earlier in this report indicate that attenuation by the flow shield is expected at these frequencies (i.e., lower amplitude measurements by the shielded hydrophone). Further inspection of the raw hydrophone data and measured calibration curves indicates that this is likely due to uncertainty in the high frequency hydrophone calibrations. Appendix D shows the same data as in Figure 6 without calibration applied (units of V) and the calibration curves measured for each hydrophone with no flow shield attached. While the amplitudes of the spectra from the two hydrophones are misaligned due to differences in sensitivity, their shapes align with expectations. Above 30 kHz, the spectra recorded by the unshielded hydrophone are relatively flat, while decreases in amplitude are observed in the spectra from the shielded hydrophone around 32, 64, and 98 kHz – the same frequencies where differences in sensitivity were observed in the calibrations conducted with flow shields attached. This, in conjunction with the nonlinear shape of the calibration curves at these high frequencies,

indicates that uncertainty in the high frequency calibration curves is likely higher than the attenuation by the flow shield.

Lastly, we can compare these results to the findings of Cotter et al. (2024). Flow noise contamination measured by the baseline hydrophone in the present study was higher than the 2024 study at the same flow speeds; this is likely a consequence of higher turbulence at the second deployment site close to the PNNL-Sequim pier. Further, flow noise reduction by the oil-filled flow shield was higher in the present study than the 2024 study. In the present study, the flow shield effectively eliminated flow noise contamination at all flow speeds measured (flow speeds < 0.7 m/s). Conversely, in Cotter et al. (2024), flow noise contamination at frequencies below 50 Hz was evident in data from the hydrophone with the oil filled shield at flow speeds above 0.4 m/s. This may be due to the larger size of the flow shield used in this study, as flow noise contamination depends on hydrophone geometry (Bassett et al. 2014). Cotter et al. (2024) used Ocean Instruments Soundtrap hydrophones, which have a smaller form factor, and therefore a smaller flow shield was used.

3.3 Durability

After the 26-day deployment, both flow shields were still filled with oil and no significant biofouling or degradation was observed. To explore survivability for longer deployments, an icListen hydrophone with a flow shield was semi-permanently installed on a piling of PNNL-Sequim's research pier on August 15, 2025. At the time of writing this report (March 2026), the hydrophone has been deployed for over six months, and no oil leakage has occurred. Divers have wiped the flow shield clean of biofouling during periodic inspections (approximately 1x/month) but have reported only minimal soft biofouling accumulation on the shield (Figure 7).



Figure 7: Pier-mounted hydrophone with flow shield upon deployment (August 2025) and during diver inspection (March 2026).

4.0 Ease of Assembly

Assembly of the original prototype oil-filled flow shield involved filling the flow shield with oil, then inserting the hydrophone and overflowing any excess oil to minimize the formation of any air bubbles. While this technique was effective, it was messy and imprecise. PNNL and XFlow investigated alternative methods for flow shield assembly that would be suitable for a commercial product. Ultimately, it was determined that the most efficient method is:

- 1) Loosely attach hose clamp to empty flow shield
- 2) Partially fill flow shield with a predetermined volume of oil; this volume will mostly fill the flow shield once the hydrophone is submerged, but will not overflow. A fill line on the flow shield can be used to indicate the initial fill volume.
- 3) Insert hydrophone and partially tighten hose clamp
- 4) Finish filling the flow shield with a flexible syringe
- 5) Tighten hose clamp and invert to test

Care should be taken to ensure that the hydrophone sensor is centered within the flow shield, as indicated by the results of calibration presented in Section 2 of this report. Detailed instructions for this procedure are included in Appendix B. We note that this assembly technique was used by Ocean Networks Canada staff with no prior experience with the flow shields when they conducted calibrations, and they reported that it was straightforward.

5.0 Conclusions

This study comprehensively evaluated the performance of an oil-filled urethane flow shield. The results indicate that the flow shield effectively reduces flow noise contamination with minimal effect on measurements at higher frequencies. Specifically, the flow shield reduced flow noise by over 20 dB at frequencies below 50 Hz while attenuating propagating sound by no more than 2 dB at frequencies below 30 kHz. The flow shield showed no signs of mechanical degradation after a 6 month deployment in a shallow tidal channel, and design refinements facilitated relatively straightforward assembly.

6.0 References

- Bassett, Christopher, Jim Thomson, Peter H. Dahl, and Brian Polagye. 2014. “Flow-Noise and Turbulence in Two Tidal Channels.” *The Journal of the Acoustical Society of America* 135 (4): 1764–74. <https://doi.org/10.1121/1.4867360>.
- Bassett, Christopher, Jim Thomson, and Brian Polagye. 2013. “Sediment-Generated Noise and Bed Stress in a Tidal Channel.” *Journal of Geophysical Research: Oceans* 118 (4): 2249–65. <https://doi.org/10.1002/jgrc.20169>.
- Biffard, Ben, Manuel Morgan, Lanfranco Muzi, Tom Dakin, and Peter Van Buren. 2022. “An Integrated Hydrophone Calibration System for Ocean Observing: ONC HydroCal.” *OCEANS 2022, Hampton Roads*, October, 1–5. <https://doi.org/10.1109/OCEANS47191.2022.9976955>.
- Cotter, Emma, James McVey, Linnea Weicht, and Joseph Haxel. 2024. “Performance of Three Hydrophone Flow Shields in a Tidal Channel.” *JASA Express Letters* 4 (1): 016001. <https://doi.org/10.1121/10.0024333>.
- Goring, Derek G., and Vladimir I. Nikora. 2002. “Despiking Acoustic Doppler Velocimeter Data.” *Journal of Hydraulic Engineering* 128 (1): 117–26. [https://doi.org/10.1061/\(ASCE\)0733-9429\(2002\)128:1\(117\)](https://doi.org/10.1061/(ASCE)0733-9429(2002)128:1(117)).
- Haver, Samara M., Jason Gedamke, Leila T. Hatch, et al. 2018. “Monitoring Long-Term Soundscape Trends in U.S. Waters: The NOAA/NPS Ocean Noise Reference Station Network.” *Marine Policy* 90 (April): 6–13. <https://doi.org/10.1016/j.marpol.2018.01.023>.
- Haxel, Joe H., and Sarah K. Henkel. 2017. *Measuring Changes in Ambient Noise Levels from the Installation and Operation of a Surge Wave Energy Converter in the Coastal Ocean*. DOE-OSUHMSC-0006387. Oregon State University, Newport, OR (United States). <https://doi.org/10.2172/1400245>.
- Martin, S. Bruce, Briand J. Gaudet, Holger Klinck, et al. 2021. “Hybrid Millidecade Spectra: A Practical Format for Exchange of Long-Term Ambient Sound Data.” *JASA Express Letters* 1 (1): 011203. <https://doi.org/10.1121/10.0003324>.
- Polagye, Brian, Corey Crisp, Lindsey Jones, et al. 2024. “Performance of a Drifting Acoustic Instrumentation SYstem (DAISY) for Characterizing Radiated Noise from Marine Energy Converters.” *Journal of Ocean Engineering and Marine Energy*, ahead of print, December 12. <https://doi.org/10.1007/s40722-024-00358-6>.
- Wahl, Tony L. 2003. “Discussion of ‘Despiking Acoustic Doppler Velocimeter Data’ by Derek G. Goring and Vladimir I. Nikora.” *Journal of Hydraulic Engineering* 129 (6): 484–87. [https://doi.org/10.1061/\(ASCE\)0733-9429\(2003\)129:6\(484\)](https://doi.org/10.1061/(ASCE)0733-9429(2003)129:6(484)).

Appendix A – Flow Shield Drawing

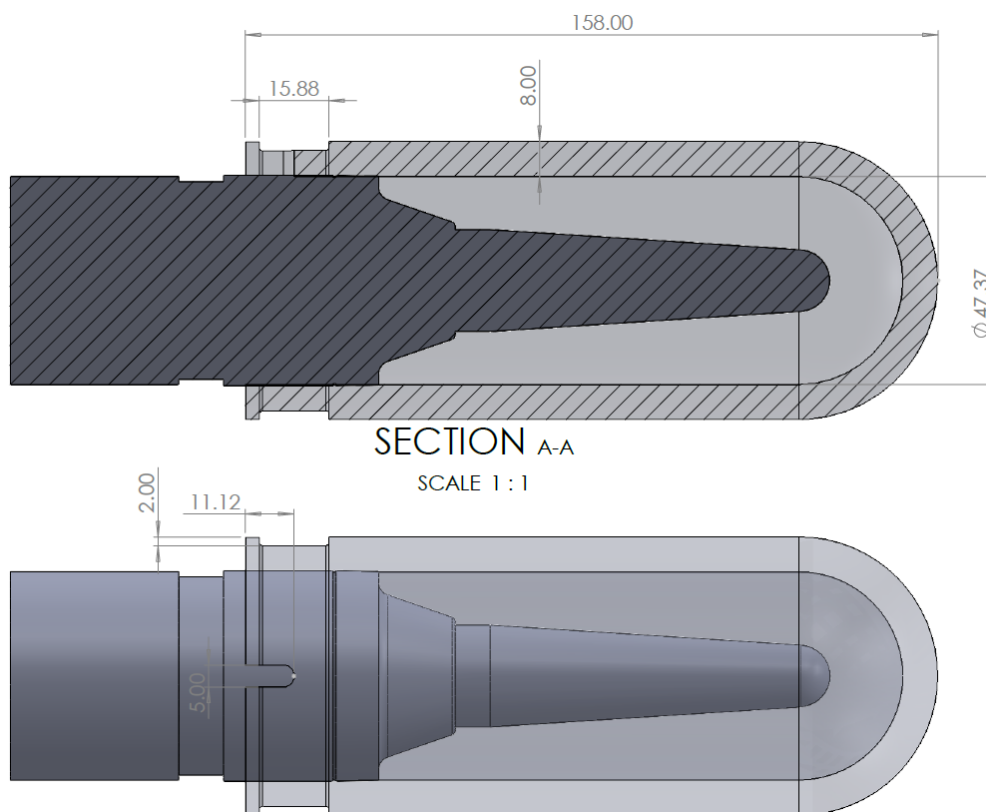


Figure 8: Dimensioned drawing of the icListen HF flow shield that was tested

Appendix B – Flow Shield Installation Instructions

Note: it is recommended to have two people available for this task.

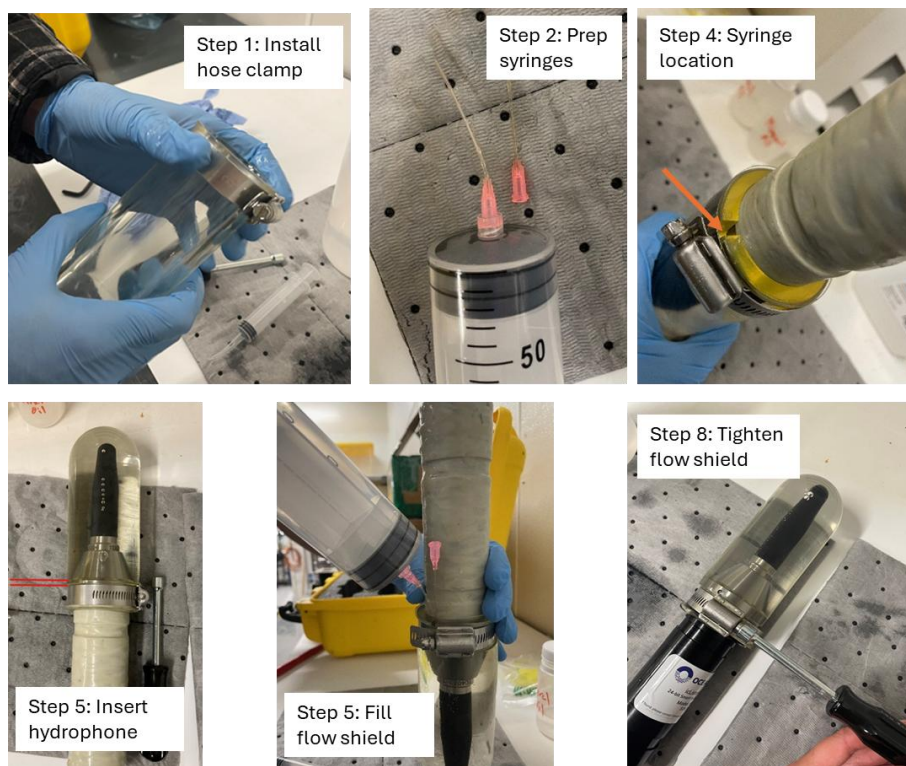


Figure 9: Photographs of key installation steps

1. Install the loosened hose clamp onto the empty flow shield.
2. Prepare the syringe by installing the tip and filling with oil for final backfill. Set one extra tip aside.
3. Fill the flow shield with mineral oil to the marked fill line (150-160 mL for an Ocean Sonics RB9 Hydrophone).
4. Have one person hold the syringe and an extra syringe tip in place in the relief in the flow shield collar (denoted by the orange arrow). The second syringe tip is to allow air to escape from the flow shield during filling.
5. The other person inserts the hydrophone into the flow shield until the shoulder is roughly 1-2mm below the bottom of the hose clamp – as denoted by the red lines.
6. Dispense oil into the flow shield to top of the remaining volume, until you see no air in the shield.
7. Lightly tighten the hose clamp to secure it in place and remove the two syringe tips.
8. Tighten the hose clamp the rest of the way to seal the flow shield. The hydrophone should be centered within the flow shield.
9. Wipe off any excess oil that is on the exterior of the flow shield and hydrophone.
10. Turn the hydrophone over and lightly squeeze the flow shield to ensure there are no oil leaks. Minimal bubbles should be present if the flow shield was secured properly.

Appendix C – Field Test Data Description and Processing

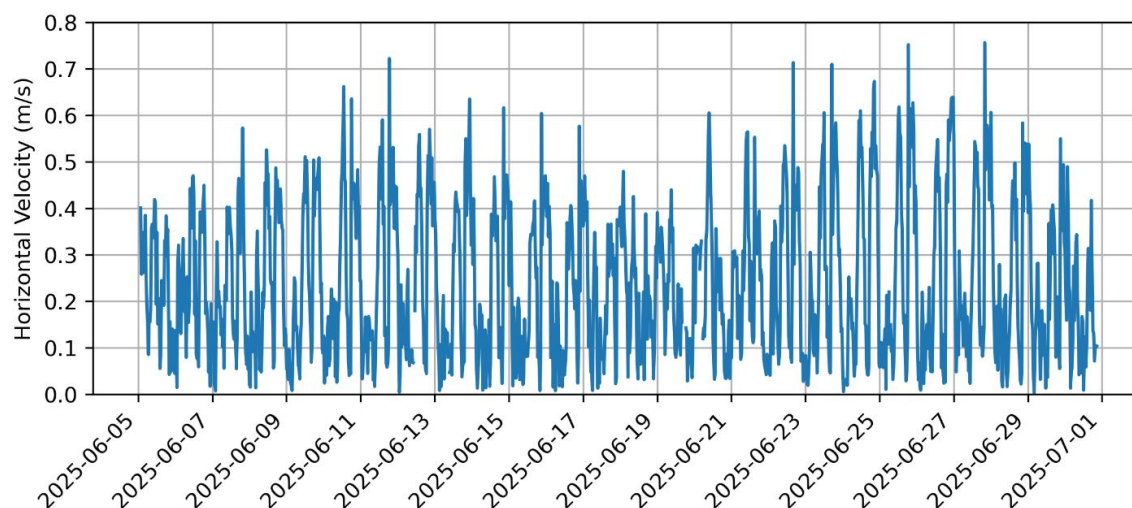


Figure 10: Timeseries of horizontal flow velocity recorded by the ADV

The hydrophones were configured to log data in 1-min duration .wav files. Logging was continuous, and data were logged on the hydrophone internal memory. Because the internal memory is limited, data were offloaded periodically to free memory space. This resulted in several 1-2 day periods of data loss due to human error in the offload procedure. Ultimately, 26,698 and 30,167 1-min files were recorded with the shielded and unshielded hydrophones, respectively. For each hydrophone file, spectrum levels were calculated in 1 s (256,000-point) windows with 50% overlap. Each window was tapered with a Hamming window before calculating the spectra using a direct Fourier transform, yielding a frequency resolution of 1 Hz. To reduce the file size and increase the speed of subsequent data processing, the spectra were averaged across millidecade bands (Martin et al. 2021) for frequencies where millidecade bands are wider than 1 Hz (>434 Hz). The resulting spectra for each .wav file were then archived as a netcdf file.

A spectrogram from each 1-min file was manually reviewed to identify time windows contaminated by noise from passing vessels, the nearby floating dock banging on the pier in boat wakes, and cobbles or other debris impacting the hydrophone lander. These files were removed from further analysis. After removing these files and limiting data analysis to only periods where data were available from both hydrophones, 17,753 1-min files remained from each hydrophone. Finally, 1-minute mean spectra were calculated for each file to create a long-term spectral average.

The ADV was configured to record for 5 min every 30 min. This sampling schedule was selected to maximize the system’s internal battery life over the course of the deployment while providing a sufficiently long sampling window for averaging. Velocity data were processed using the Doppler Oceanography Library for Python (DOLfYN)¹. Data were “de-spiked” following Goring and Nikora 2002 and Wahl 2003 using a window size of 5000 points, and data points with correlation values lower than 70% were also removed. Removed data points were filled using cubic spline interpolation before calculating the mean velocity for every 5-min recording window. The resulting time series of flow velocity is shown in **Error! Reference source not found.** F

¹ <https://mhkit-software.github.io/MHkiT/dolfyn.html>

inally, the flow speed during each 1-minute hydrophone recording window was then estimated using linear interpolation.

Appendix D – Hydrophone Calibration Uncertainty

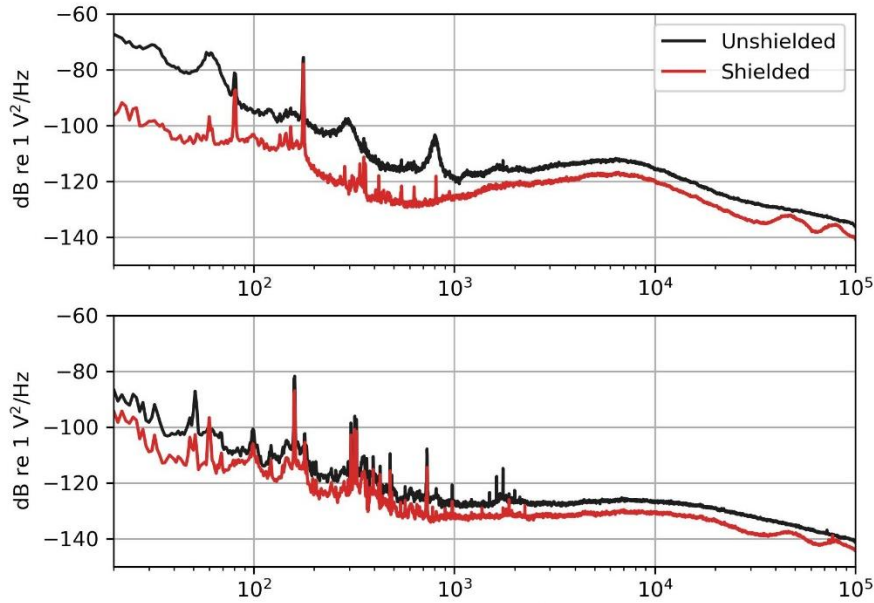


Figure 11: The same data as shown in Figure 6 before applying calibration curves to convert to units of pressure

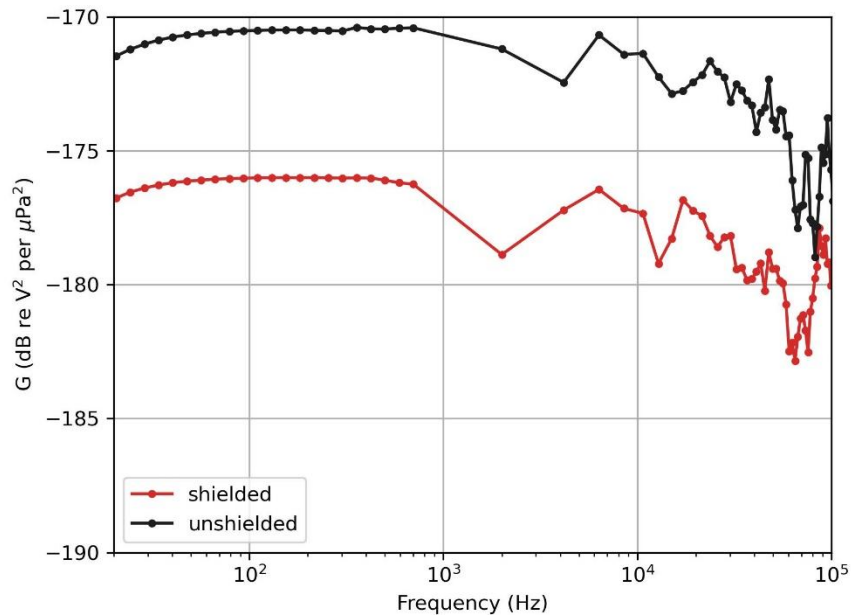


Figure 12: Calibration curves for each hydrophone used in the field trial to convert from units of V to units of pressure. Calibration curves were measured with no flow shield attached.

Pacific Northwest National Laboratory

902 Battelle Boulevard
P.O. Box 999
Richland, WA 99354

1-888-375-PNNL (7665)

www.pnnl.gov